2013 IEEE/RSJ International Conference on
Intelligent Robots and Systems (IROS)
November 3-7, 2013. Tokyo, Japan

Design and Control of a Spherical Omnidirectional Blimp

M. Burri, L. Gasser, M. Käch, M. Krebs, S. Laube, A. Ledergerber, D. Meier, R. Michaud, L. Mosimann, L. Müri, C. Ruch, A. Schaffner, N. Vuilliomenet, J. Weichart, K. Rudin, S. Leutenegger, J. Alonso-Mora, R. Siegwart, P. Beardsley

Abstract— **This paper presents Skye, a novel blimp design. Skye is a helium-filled sphere of diameter 2.7m with a strong inelastic outer hull and an impermeable elastic inner hull. Four tetrahedrally-arranged actuation units (AU) are mounted on the hull for locomotion, with each AU having a thruster which can be rotated around a radial axis through the sphere center. This design provides redundant control in the six degrees of freedom of motion, and Skye is able to move omnidirectionally and to rotate around any axis. A multi-camera module is also mounted on the hull for capture of aerial imagery or live video stream according to an 'eyeball' concept - the camera module is not itself actuated, but the whole blimp is rotated in order to obtain a desired camera view.**

Skye is safe for use near people - the double hull minimizes the likelihood of rupture on an unwanted collision; the propellers are covered by grills to prevent accidental contact; and the blimp is near neutral buoyancy so that it makes only a light impact on contact and can be readily nudged away.

The system is portable and deployable by a single operator - the electronics, AUs, and camera unit are mounted externally and are detachable from the hull during transport; operator control is via an intuitive touchpad interface.

The motivating application is in entertainment robotics. Skye has a varied motion vocabulary such as swooping and bobbing, plus internal LEDs for visual effect. Computer vision enables interaction with an audience. Experimental results show dexterous maneuvers in indoor and outdoor environments, and non-dangerous impacts between the blimp and humans.

I. Introduction

This paper describes the design of Skye blimp, presents experiments to demonstrate its capabilities under manual control, describes the potential for flying autonomously, and shows its suitability for safe deployment near people.

The design is symmetrical with a spherical hull, four tetrahedrally arranged thrusters, and the center of gravity (COG) close to the center of the sphere. There is no preferred orientation or forward direction. The blimp is capable of holonomic motion, able to translate in any direction and to rotate around any axis independently. The design supports flexible capture of aerial imagery according to an eyeball concept - the camera module is fixed on the hull, and the blimp is positioned and oriented as desired to obtain a required camera view.

There is growing interest in low-cost unmanned aerial vehicles (UAV) such as quadrotors and hexacopters across multiple domains - professional, hobbyist, and as toys. This is bringing multicopters into closer proximity with people and motivating a need for new safety concepts. Multicopter safety can be achieved by low weight, propeller guards, propeller auto-stop on obstruction, and autonomy if a manual RC signal is lost. Low weight is achievable with quadrotors as consumer product, but applications which require hardware such as cameras, on-board storage, a wireless module, and an on-board processor, can easily result in a payload of 500g and more. This is sufficient to cause injury if there is a loss of control that causes the multicopter to fly into or fall on a person. The problem is circumvented by a helium blimp with neutral buoyancy. The worst-case failure scenario for a blimp would be rupture of the hull, but this can be minimized by a double hull like the design here. Skye's propellers have a protection ring and a nylon grill to prevent accidental contact.

The application is entertainment robotics. Some existing examples of entertainment blimps have unusual shapes such as jellyfish [1] or sharks [2]. Skye is a sphere and one goal is to achieve entertaining effects using versatile motion and eye-catching hull pattern. Internal LEDs enable nighttime aesthetic effects, related to fireworks. Multiple blimps can be choreographed in a collision-free aerial display using the method described in [4]. A further goal is interaction, for example to automatically detect gestures of individuals or crowds using the onboard camera, to enable aerial games.

A. Related Work

Sharf [5], [6] presented a spherical indoor blimp to emulate a free floating object in a gravity-free environment. Like Skye, it is able to perform six degrees of freedom motions but achieves this by using six instead of Skye's four propellers. It is smaller than Skye with a diameter of 1.8m, but bound to indoor use and limited payload. Minizepp [7] developed a series of indoor and outdoor blimps capable of aerial imagery, which inspired Skye's double hull. In recent years bigger airships, suitable for intelligence gathering and information transferring, experienced a renaissance. Unlike Skye these airships are not meant to fly closely to objects and people, but rather to operate in high altitude. Therefore more emphasis is put on payload than on size and agility. An example of such an airship is LEMV [8] (Long Endurance Multi-Intelligence Vehicle) a recently developed hybrid airship for surveillance operations which demonstrates the continued advantage of airships for long deployment. Another project focusing on long deployments and high altitudes is the SA-60 [9] developed by Techsphere Systems International. With the ability

M. Burri, L. Gasser, M. Käch, M. Krebs, S. Laube, A. Ledergerber, D. Meier, R. Michaud, L. Mosimann, L. Müri, C. Ruch, A. Schaffner, N. Vuilliomenet, J. Weichart, K. Rudin, J. Alonso-Mora, S. Leutenegger, R.Siegwart are with the Autonomous Systems Lab, ETH Zurich, 8092 Zurich, Switzerland makrebs@student.ethz.ch

J. Alonso-Mora, P. Beardsley are with Disney Research Zurich, 8092 Zurich, Switzerland {jalonso,pab}@disneyresearch.com

to carry a pilot and a passenger this spherical airship is much bigger than Skye, diameter 18.9m compared to Skye's 2.7m. The spherical shape was chosen to reach high altitudes, to present the wind the same aspect ratio for all directions and to get a small footprint. However, its motions are restricted as it uses only two main engines for propulsion. Focusing more on airship control than on design, Fernandez [10] developed a comprehensive model for a non-spherical indoor blimp with which different autonomously controlled navigation techniques could be evaluated. Using electro-active polymers for propulsion, Jordi [11] demonstrated a fishlike airship. ODIN [12] is a spherical autonomous underwater robotic vehicle capable of six degrees of freedom motions. This is achieved by eight thrusters in a planar configuration and one finlike manipulator.

B. Contribution

Our contribution is a novel blimp design which is capable of holonomic motion in an indoor and outdoor environment. The most closely related work is Sharf [5], [6] in which the blimp's center of buoyancy is close to the COG. This is energy efficient because it avoids the need to correct for a residual momentum which causes the COG to fall to the lowest point. However, our design demonstrates the concept with four instead of six thrusters. This leads to reduced thruster noise around people as an advantage for entertainment and lower energy usage, hence longer flight times. A second contribution is to show that the proposed design is the most suitable arrangement for omnidirectional flight while maintaining evenness of efficiency in all directions, as discussed in Section III-B. Finally from an application perspective, Skye's design provides a flexible platform for entertainment experiences, offering a versatile motion vocabulary such as spinning and bobbing, safety near people, interaction via computer vision, and portability of the deflated system in a packing case.

II. Overview

Figure 1 shows a system overview. Skye consists of a double layer spherical hull filled with helium, providing sufficient lift for the system to have neutral buoyancy. For convenience, slight negative buoyancy guarantees automatic return to ground when the thrusters are stopped. Each of the four tetrahedrally arranged actuation units are attached by Velcro and provide thrust tangentially to the hull and are fully rotatable. All electronic components are concentrated to one central point on the surface of the hull in order to reduce cable weight. This cluster includes GPS and IMU units to enable controlled maneuvers. One high resolution camera plus two low resolution cameras provide a basis for human interaction and computer vision, as well as live stream for piloting the system. The power is provided by three accumulators. There are four handles sewn to the hull for manipulation and ground attachment. The arrangement of components is chosen such that the center of gravity lies approximately in the center of the sphere. Therefore the system ideally retains its orientation passively.

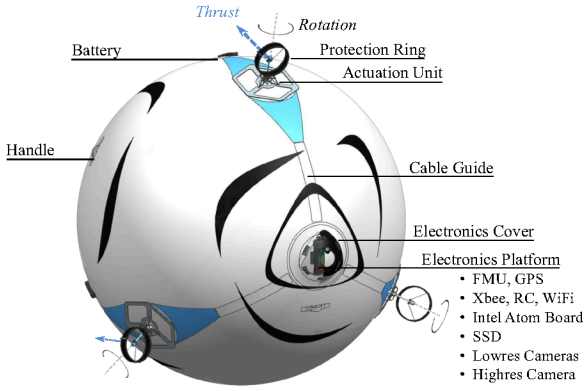

Fig. 1. Overview of blimp components - electronics, AUs, and camera module are all detachable from the hull. Propellers have a protection ring and nylon grill.

III. System

A. Hull

The envelope is an integral part of the airship structure and carries all components - electronics, actuation units, camera module, accumulators and the corresponding cables. The outer layer of the blimp hull is realized with a nylon (PA 6.6) fabric which is strong, almost inextensible and sewn. It is combined with an inner polyurethane (PU) membrane which is helium tight and very elastic. By applying overpressure a hard and form stable hull is obtained. The wires are guided through cable channels which are sewn into the hull. The other components are removable and are attached by Velcro. As no rigid structure connects the individual AUs, a design criterion was defined - the bending of the actuation unit due to full thrust caused by hull deformation must be smaller than one degree. To transmit the thrust force uniformly to the envelope and to keep stress peaks in the fabric small, a baseplate was designed at the interface between AU and hull (see figure 2).

The design criterion relates the size of the baseplate with the overpressure where the plate radius r is defined in dependency of the overpressure Δp. The maximal thrust force F_{th} of an AU multiplied with its orthogonal distance h from the hull surface yields the bending moment and $\alpha_{max} = 1^\circ$ is the maximal deformation: $r^2 \Delta p > \frac{hF_{th}}{\alpha_{max} r}$.

To reduce the size of the baseplate (which is related to weight) higher overpressure must be present to fulfil the requirement. However, the overpressure is limited to 70 mbar by the strength of the nylon fabric. Therefore the initial operation pressure must be significantly smaller than this limit as the inner pressure depends highly on environmental conditions such as temperature or outer pressure.

B. Actuation

An actuation unit consists of a propeller for thrust generation which is mounted on a rotatable shaft. The torque for the

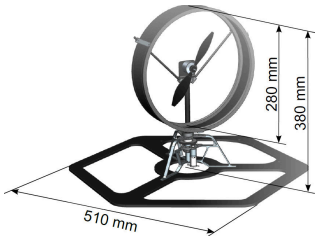

Fig. 2. A safety ring shields the propeller. It is stringed with threads to prevent fingers touching the blade. The lower part of the model shows the turning motor safely placed within the weight optimized aluminium frame.

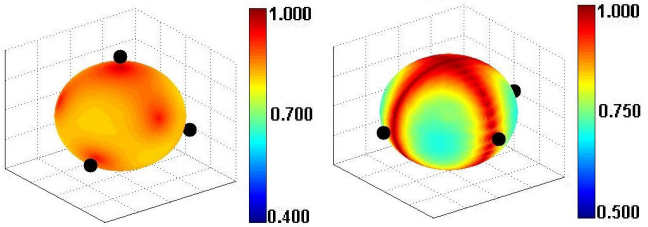

Fig. 3. Plot of the effectiveness η in all spherical directions for the tetrahedral actuation arrangement (left) and a planar placement as a reference (right).

rotation is provided by a maxon servomotor and transmitted to the shaft by a gear mechanism. This construction enables an unlimited number of revolutions. The electric current and the signals for the thrust motor and controller are transmitted over a slip ring which has to be in axes with the shaft. After system start, all actuation units automatically go to a defined position using a light barrier sensor.

The goal was to find the most suitable arrangement of these AUs for omnidirectional flight properties maintaining high efficiency in all directions. To compare them two characteristic values were considered. For sake of simplicity, only geometric constraints are considered, i.e. a perfect force model is assumed. The translational effectiveness η is the absolute value of the resulting force divided by the sum of the absolute values of the thruster forces.

$$\eta = \frac{|F_{res}|}{\sum_i^N |F_i|} \tag{1}$$

A plot of η in all directions for a tetrahedral arrangement of the AUs is shown if figure 3. As a reference, the plot for a planar arrangement of four AUs is depicted too.

$\sigma \in [1,N]$ is a way of measuring how much of the resulting thrust must be contributed by one single motor:

$$\sigma = \frac{|F_{res}|}{max_i\,(|F_i|)} \tag{2}$$

A σ of 1 indicates that the whole thrust is generated by one motor where a σ of N denotes that all motors contribute equally with $|F_i|/|F_{res}| = 1/N$ each (e.g. $|F_i| = 0.25|F_{res}|$ for $N = 4$).

The tetrahedral solution was found to be the most suitable to fulfill the requirements of omnidirectional motion. Additionally it has also the best *worst directions* of the considered arrangements.

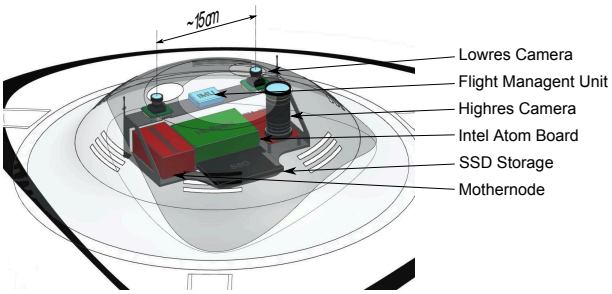

Fig. 4. Schematic illustration of the central electronics platform including control, camera and storage devices.

C. Electronics and Camera Module

All electronic components are attached on the surface of the hull. The AUs are controlled by the central flight management unit (FMU) from pixhawk [15] located at the electronics platform (see figure 4). It incorporates a 3D accelerometer, gyroscope, magnetometer and a pressure sensor as well as a local 168MHz processing unit where the control loop is running. Furthermore, a u-blox GPS-receiver is connected.

To address the AUs a communication system on the blimp is required. It is implemented as a customized differential RS485 bus system. This tailored solution allows a slim realization of the cables and its differential format ensures reliable data transmission over the large distances between the nodes.

A LED chain is clutched straight through the inside of the hull. A wire leads out through the hull outlet and is connected to an AU. The chain is powered via a DC-to-DC converter placed on an AU's electronics board. An I2C bus is used to control the LED color, which can be chosen by the pilot on a color panel on the GUI. It is transmitted via the same channels as motion control inputs.

Skye carries two low resolution cameras (MV BlueFox MLC200wC) with a baseline of approximately 15cm and a high resolution camera (AVT Prosilica GB2450C) located near the BlueFox as it can be seen in figure 4. All pictures captured are processed on a high level board (Pico ITX board with Intel Atom processor 510D 1.66GHz) and stored on an on-board solid state disk (SSD) while a WiFi module enables a live stream to enhance piloting.

D. System Dynamics

Due to the six DOF of Skye in 3D space and numerous unpredictable disturbances, a direct control of the system is not sufficiently intuitive. Therefore, a control algorithm (see section III-E) has been designed to make piloting feasible. For a better understanding of the system dynamics and to be able to develop a controller prior to the completed construction of the prototype, a model was implemented in MATLAB SIMULINK as shown in figure 5.

The system dynamics were modeled assuming rigid bodies. To describe the system state, both a body frame (denoted by ${}_B(.)$) and an inertial frame (denoted by ${}_I(.)$) are used as they are visualized in figure 6.

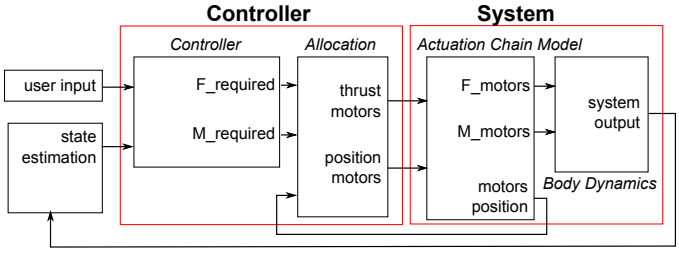

Fig. 5. Closed loop control system in MATLAB SIMULINK

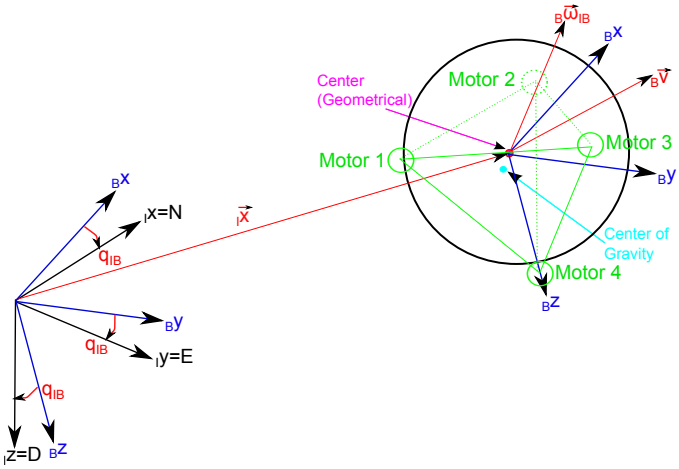

Fig. 6. Visualization of the used coordinate systems and the states (red).

To describe the state of the system the four vectorial equations (3-6) are used. Gravity and aerodynamical effects were also included but are not discussed further. The translational velocities result from the principle of linear momentum:

$$\frac{d}{dt}{}_B\vec{v}_{CG} = \underline{\underline{m}}_{tot}^{-1} \cdot {}_B\vec{F}_{tot,CG} - {}_B\vec{\omega}_{IB} \times {}_B\vec{v}_{CG} \ , \tag{3}$$

where ${}_B\vec{F}_{tot}$ is the resulting force (the sum of the forces generated by the rotors, gravitational forces and forces generated by aerodynamic effects), $\underline{\underline{m}}_{tot}$ the mass matrix including aerodynamical effects and ${}_B\vec{v}_{CG}$ the velocity of the center of gravity.

The position can be calculated by integrating the velocity vector in the inertial system:

$$\frac{d}{dt}{}_I\vec{x}_{O-CG} = {}_I\vec{v}_{CG} \tag{4}$$

The angular velocities are evaluated with the principle of angular momentum:

$$\frac{d}{dt}{}_B\vec{\omega}_{IB} = {}_B\underline{\underline{J}}^{-1} \cdot \left({}_B\vec{M}_{tot,CG} - {}_B\vec{\omega}_{IB} \times \left({}_B\underline{\underline{J}} \cdot {}_B\vec{\omega}_{IB} \right) \right) \tag{5}$$

where ${}_B\vec{\omega}_{IB}$ is the angular velocity, ${}_B\underline{\underline{J}}$ the inertia tensor and ${}_B\vec{M}_{tot,CG}$ the resulting moment in the center of gravity. The orientation is given by the unit quaternion $\vec{q}_{IB}$ which describes the rotation of the body relative to the inertial frame. Its change is defined by the angular velocity $\vec{\omega}_{IB}$:

$$\frac{d}{dt}\vec{q}_{IB} = \frac{1}{2}\vec{q}_{IB} \otimes \begin{pmatrix} 0 \\ {}_B\vec{\omega}_{IB} \end{pmatrix} \tag{6}$$

.

E. Control Algorithm

The control algorithm has been split into two parts to allow a more intuitive design of the code (see figure 5). The first part of the controller determines the required force and moment. The state feedback is a quaternion calculated by an Extended Kalman Filter (EKF) proposed by Leutenegger [14]. The second stage is the conversion of force and moment into thrust and position of the AUs, referred to as allocation.

The control strategy follows a hierarchical structure, beginning with the state feedback linearization of the velocity and angular velocity equations to decouple translations from rotations by eliminating the cross product terms. While the attitude equation is linearized by the Jacobian, the position equation is simply used in the inertial frame, where it appears in its linear form. The resulting control problem is then solved by the implementation of two sets of cascaded control loops consisting of an inner P and outer PI regulator for position and velocity, as well as attitude and angular velocity. A differential part is not implemented since the inner loop implicitly acts as a derivative part for the outer loop in cascaded loop strategies (see figure 7).

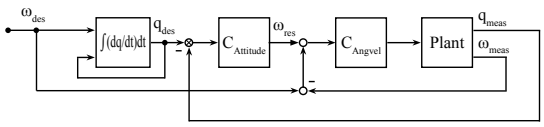

Fig. 7. Cascaded control structure with angular velocity controller and attitude hold block.

With this method the controller determines the optimal force and momentum to act on the COG of the system. As the actuation performance is limited, anti integral windup and restriction loops were implemented such that the controller does not request actuation values beyond the systems capabilities.

The allocation calculates the signals for the positioning and thrust motors. As the system has eight inputs (thrust F_i and direction α_i for each AU), two degrees of freedom can be used for an optimization of the signals for the motors. In order to simplify the allocation of the actuators the following assumptions were made:

- Negligible thrust motor dynamics: It is supposed that the thrust motor can reach every rotational speed within a certain range immediately.
- Linearized positioning motor dynamics: Neglecting acceleration (and deceleration) the required time to sweep a certain angle is linear to the angle offset.
- Negligible drag torque: The drag torque of the propeller is about a hundred times smaller than the torque resulting from the thrust force.
- Linear thrust approximation: A linear function was fitted experimental results to relate the thrust motor signal to the thrust force.

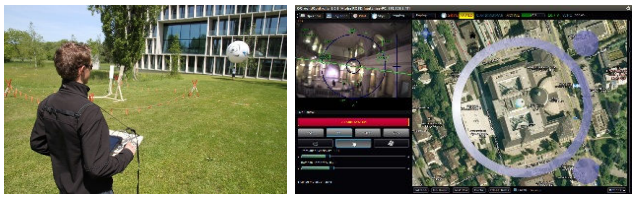

Fig. 8. **Left:** Portable setup for tablet and 3D mouse. **Right:** Tablet GUI with rotational touch area on the live stream (top left), translational touch area on the map (right), and control panel for flight modes (bottom left).

By using a standard DC motor model and the Blade Element Momentum Theory [13] for the modeling of the actuation unit, the relationship between the motor inputs (the thrusters voltage V_i and the current orientation angle α_i) and the resulting thruster force vector $\vec{F}_i$ was determined. On this basis, a static allocation was developed that converts the six controller outputs $\vec{F}_s$ and $\vec{M}_s$ into the motor signals V_i and α_i. This optimization problem was solved using Lagrange multipliers with linear equality constraints and an objective function chosen to minimize the overall power consumption, i.e. it is the sum of the absolute value of the thruster force vectors:

$$f = \sum_{i=1}^{4} ||\vec{F}_i||^2 \tag{7}$$

Since only its derivative appears in the Lagrange equation, the solution becomes linear.

F. Piloting

Manual control is achieved using a Lenovo ThinkPad X220t tablet computer plus SpaceNavigator 3D mouse by 3dConnexion to control the six DOF of motion. The mouse allows for separate control of translation and rotation. Portability of the system is achieved using a neck lanyard with carrying platform as shown in figure 8 (left). The graphical user interface shows the live stream, the current attitude and position of the blimp, and a map as shown in figure 8 (right). Touch on the live stream on the tablet can be used to direct the camera as shown in figure 9. Manual inputs are interpreted as desired velocity or angular velocity respectively. Therefore, the position and orientation reference for the system will be achieved as a result of the integrated inputs.

The control commands and telemetry data are transmitted via a Xbee 2.4GHz device. Live stream is transmitted by WiFi 802.11n 5GHz. A common RC device with two sticks (e.g. Futaba C7) transmitting via a redundant communication channel can be used to control 4 DOF, i.e. three rotative and one translational motion. This device is a redundant back up system in case of communication loss between tablet and blimp.

IV. Results

This section describes the physical system and experimental results. The work so far represents a first stage of development, including significant usage experience and some quantitative analysis. A full quantitative analysis will be the main topic for future work.

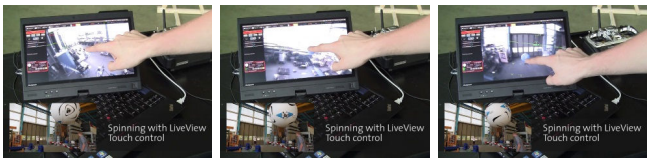

Fig. 9. Intuitive interface to implement the blimp's eyeball concept - the blimp camera is directed at an object of interest by touching the object on the live camera view.

A. Weight and Buoyancy

The blimp is a sphere with diameter 2.7m and total mass of around 9.5kg. The weights of the individual components are

- hull - 3.65kg
- AU (each) - 0.64kg
- battery total - 1.75kg
- cables - 0.58kg
- camera module - 0.95kg

Buoyancy is dependent on the environmental temperature and ambient pressure. Tuning weights are attached or removed to each AU to adjust the buoyancy while maintaining the position of the COG. The deflated blimp and components can be packed in a box of 600x600x500mm for easy portability.

B. Qualitative Results

This section describes qualitative results relevant to our target applications. The blimp has been tested in both indoor and outdoor environments with light winds up to 12 km/h. Above this speed, the wind disturbance exceeds the actuation constraints. Figure 10 shows the following tests:

(a) Translation at 20 km/h
(b) Rotation at 0.5 rev/s
(c) Circumnavigation of a tall tree
(d) Safe and easily-deflected contact with a human

A video showing these experiments can be found in [16].

Figure 11 shows the system flying in an inner courtyard above a crowd. The blimp can be flown at touching distance above crowds, allowing individuals to deflect it in different directions. Figure 12 shows Skye with a printed moon hull - one hemisphere has a cratered surface while the reverse hemisphere is black. Internal LEDs provide a glow. The advantage of versatile motion can be seen in an aerial display where the blimp rises and sets over an audience while rotating to demonstrate the moon's phases.

C. Quantitative Results

Flight time depends on multiple parameters. Operation times of more than two hours are achieved while continuously performing low-speed maneuvers in a wind protected place.

Fig. 10. Qualitative results obtained for outdoor deployment. **(a)** Translation at 20km/h. **(b)** Rotation at 0.5 rev/s. **(c)** Circumnavigating a tree. **(d)** Safe and easily-deflected contact with a human.

Fig. 11. Safe operation over crowds.

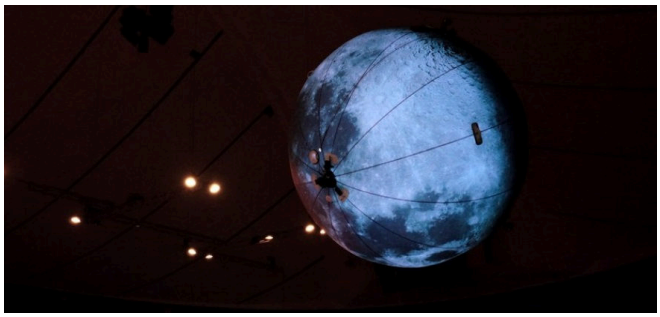

Fig. 12. Skye as the moon. A printed hull and internal LEDs enable nighttime aesthetic effects.

Quantitative results are provided for the adherence of the blimp to a specified rotational motion. The input angular velocity is compared with the angular velocity estimated by the sensor system. Figure 13 shows results achieved by a cascaded attitude controller by applying a sinusoidal angular velocity input in the z-direction. The controller was implemented according to the method described in Section III-E. Controller gains were found by respecting the crossover frequency ω_c, which is, as a rule of thumb, set two octaves below the characteristic frequency ω_{char}. The characteristic frequency is given by the time $T_{char} = 0.31$s used to orient the thrusters into the opposite direction. Therefore

$$\omega_c = \frac{\omega_{char}}{4} = \frac{\pi}{4 \cdot T_{char}} \tag{8}$$

which was found to be 2.5rad/s. Accordingly, the controller gains used were $k_{p,\omega} = 2.5$ for the inner P controller, and $k_{p,\phi} = 0.25, T_{I,\phi} = 4$s for the outer PI control loop.

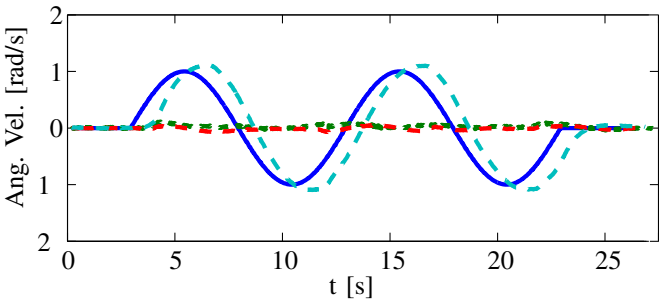

Fig. 13. System response of all angular directions x, y, z to a sinusoidal angular velocity input in only one angular direction z. ω_z input [blue], ω_x [red dashed], ω_y [green dashed], ω_z [cyan dashed].

D. Interaction using Computer Vision

An example interaction with an audience on the ground is to detect areas of large motion in the camera image, and then respond, for example, by approaching and circling that place. Figure 14 shows the detected motion for an individual who is jumping. The vision system utilizes a standard approach. The processing steps, which can be found individually in [17], are

- Determine the epipolar geometry of successive frames in an image sequence by feature detection and correspondence matching, using a method that is robust to the presence of independent motion
- Detect features with independent motion by testing for matched features that disagree with the epipolar geometry
- Group features with independent motion into blobs using mathematical morphology
- Take the largest blob as the target for the subsequent interaction

V. Conclusion and Future Work

This paper has presented Skye, a spherical helium blimp capable of holonomic motion that is suitable for entertainment applications close to people. The paper presented qualitative results plus initial quantitative analysis. A full quantitative analysis is the topic of the next stage of work.

Fig. 14. Computer vision algorithm to detect a waving user. From left, one frame of a captured sequence, detected motion, detected rectangle of largest motion.

The work can be considered in the context of recent interest in using quadrotors to make flying displays. Quadrotors are capable of fast and versatile motion, but there are currently safety challenges in placing them overhead or close to people, requiring further research to resolve. In contrast, Skye has been safely deployed within touching distance of crowds of people - the blimp is near neutral buoyancy and can be readily pushed away, and the propellers are protected by a nylon grill. As a further advantage for human settings including entertainment, the blimp has quiet operation - lifting force is delivered by the helium and thrust is selectively activated only as needed for a desired motion or to counteract wind disturbances. This also has the consequence that Skye has a longer operation time than conventional quadrotor systems.

Illuminated with internal LEDs, the blimp provides an attractive nighttime display in the same spirit as fireworks. The onboard camera and processor supports interactive games based on individual gesture or crowd motion. In conclusion, Skye is intended to be a flexible platform for aerial display and for interactive games.

REFERENCES

[1] Festo AirJelly, festo.com/cms/en_corp/9771.htm
[2] AirSwimmers, airswimmersworld.com
[3] O. Bimber, D. Iwai, G. Wetzstein, A. Grundhoefer, The Visual Computing of Projector-Camera Systems, Computer Graphics Forum, 2008.
[4] J. Alonso-Mora, M. Schoch, A. Breitenmoser, R.Y. Siegwart, P. Beardsley, Object and Animation Display with Multiple Aerial Vehicles: Proc. of the IEEE/RSJ International Conference on Intelligent Robots and Systems (IROS), 2012
[5] I. Sharf, B. Laumonier, M. Persson, J. Robert, Control of a fully-actuated airship for satellite emulation: International Conference on Robotics and Automation (ICRA), May 2008
[6] S. Mikael Persson, I. Sharf, Dynamics, Stability and Control of Indoor Spherical Airship: 7th European Nonlinear Dynamics Conference, July 2011
[7] Minizepp, minizepp.com
[8] U.S. Army LEMV, http://www.northropgrumman.com/Capabilities/lemv
[9] SA-60, http://defensetech.org/2004/07/06/blimpball-in-navy-tests/
[10] J.P. Fernandez, P. Gonzalez, R. Sanz, W. Burgard, Developing a Low-Cost Autonomous Indoor Blimp: Journal of Physical Agents, vol 3 no 1, 2009.
[11] C. Jordi, S. Michel, N. Widmer, V. Frohne: Body segment of an active airship based on dielectric elastomers: 19th International Conference on Adaptive Structures and Technologies, Ascona, Switzerland, 2008.
[12] S. K. Choi, J. Yuh: Design of Advanced Underwater Robotic Vehicle and Graphic Workstation: Autonomous Systems Laboratory, University of Hawaii, IEEE 1993
[13] A.R.S Bramwell, G. Done, D. Balmford, Helicopter Dynamics: Butterworth-Heinemann, 2nd edition, 2001.
[14] S. Leutenegger, R.Y. Siegwart, A Low-Cost and Fail-Safe Inertial Navigation System for Airplanes: International Conference on Robotics and Automation (ICRA), 2012
[15] Pixhawk, pixhawk.ethz.ch
[16] Project Skye, www.skye.ethz.ch
[17] R. Hartley, A. Zisserman, Multiple View Geometry in Computer Vision, Cambridge University Press, 2004.